Poisson's Equation with Delta Function

Zeyu Xiong, Xiaohan Li, Jessica Flores

May 14, 2019

Abstract

Poisson's equation is widely used in engineering, including fluid mechanics, heat and mass transfer, beam and plate structures, and environmental science. Therefore, engineers have developed various numerical methods to solve Poisson's equation accurately. In this project, we solved Poisson's equation with a Dirac delta function source in 2D with homogeneous Dirichlet boundary conditions using different numerical methods. These include Chebyshev spectral method, finite element method, and finite difference. The approach for approximating the delta function utilized with the various solution methods is a Gauss function as σ approaches zero. The advantages and disadvantages of each of the different solvers are compared in terms of accuracy and convergence rate.

1 Introduction

Poisson's equation is widely used in engineering, including fluid mechanics, heat and mass transfer, beam and plate structures, and environmental science. The objective of this study is to solve the 2D Poisson's equation (an elliptic PDE) with a delta function source and homogeneous Dirichlet boundary conditions using various numerical methods and approaches for approximating the delta function. Physically, this could represent the electric potential due to a point charge sitting inside a 2D conducting box.
In other words, find $u \in \Omega = [0,1] \times [0,1]$ such that for $f(x,y) = \delta(x-a,\ y-b)$, we have

$$-\Delta u = f \quad \forall\, x, y \in \Omega$$

and

$$u = 0 \quad \forall\, x, y \in \partial\Omega.$$

The Dirac delta function has some unique properties in that its value is equal to infinity at the origin and zero elsewhere. In two dimensions centered at a point (a,b), it is:

$$\delta(x-a, y-b) = \begin{cases} \infty & \text{for } x = a,\ y = b \\ 0 & \text{elsewhere} \end{cases}$$

Integrating the product of the delta function and another function results in the value of the function evaluated at the point in which the delta function is centered at:

$$\iint_{\Omega} \delta(x-a, y-b) f(x,y) dxdy = f(a,b) \quad \forall\, \Omega \in (a,b)$$

The analytical solution to this problem is then:

$$u(x,y) = -\sum_{j=1}^{\infty} \sum_{k=1}^{\infty} C_{jk} \sin(j\pi x) \sin(k\pi y)$$

where

$$
\begin{aligned}
C_{jk} &= \frac{-4}{\pi^2(j^2+k^2)} \int_0^1 \int_0^1 f(x,y) \sin(j\pi x) \sin(k\pi y) dxdy \\
&= \frac{-4}{\pi^2(j^2+k^2)} \int_0^1 \int_0^1 \delta(x-a,\ y-b) \sin(j\pi x) \sin(k\pi y) dxdy \\
&= \frac{-4}{\pi^2(j^2+k^2)} \sin(j\pi a) \sin(k\pi b)
\end{aligned}
$$

The exact solution to this problem with the point source at the center of the domain can be seen in Figure 1, where there is a singularity at point $(0.5, 0.5)$ in which the value tends to infinity. Using (a,b)=(0.5,0.5), the even terms in the sum are all zero, thus:

$$
\begin{aligned}
u(x,y) &= -\sum_{j=1}^{\infty} \sum_{k=1}^{\infty} C_{jk} \sin(j\pi x) \sin(k\pi y) \\
&= -\sum_{j=1}^{\infty} \sum_{k=1}^{\infty} \frac{-4}{\pi^2(j^2+k^2)} \sin\left(j\frac{\pi}{2}\right) \sin\left(k\frac{\pi}{2}\right) \sin(j\pi x) \sin(k\pi y) \\
&= -\sum_{j=1}^{\infty} \sum_{k=1}^{\infty} \frac{-4}{\pi^2((2j-1)^2+(2k-1)^2)} \sin\left((2j-1)\frac{\pi}{2}\right) \sin\left((2k-1)\frac{\pi}{2}\right) \sin((2j-1)\pi x) \sin((2k-1)\pi y)
\end{aligned}
$$

The plots below use the above equation with $j = 1, \ldots, 100$ and $k = 1, \ldots, 100$.

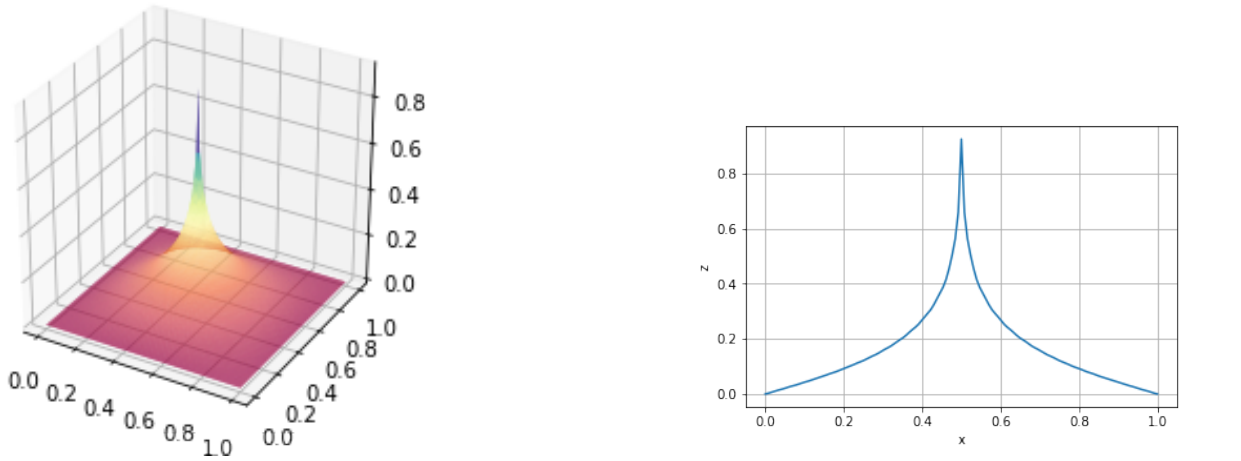

Figure 1: Analytical solution to the Poisson problem with a dirac delta function at the center of the domain.

This problem was chosen because the known true PDE solution allows for a direct computation of the error against the approximated solutions using various numerical methods.

2 Dirac Delta Function representations

There are many different methods to represent the delta function numerically, such as those shown in Figure 2. For example, a 2D step function (which is discontinuous), a 2D pyramid function (which is continuous, but not differentiable everywhere), and a Gaussian/Normal distribution (which is continuous and continuously differentiable) could be used. For ease of comparison between numerical methods, a

Gaussian function in 2 dimensions, given by the equation:

$$\frac{1}{2\pi\sigma^2}\exp\left[-\frac{(x-0.5)^2+(y-0.5)^2}{2\sigma^2}\right]$$

was chosen to represent the delta function and the parameter σ is varied. In the limit as σ approaches zero, this function produces the delta function.

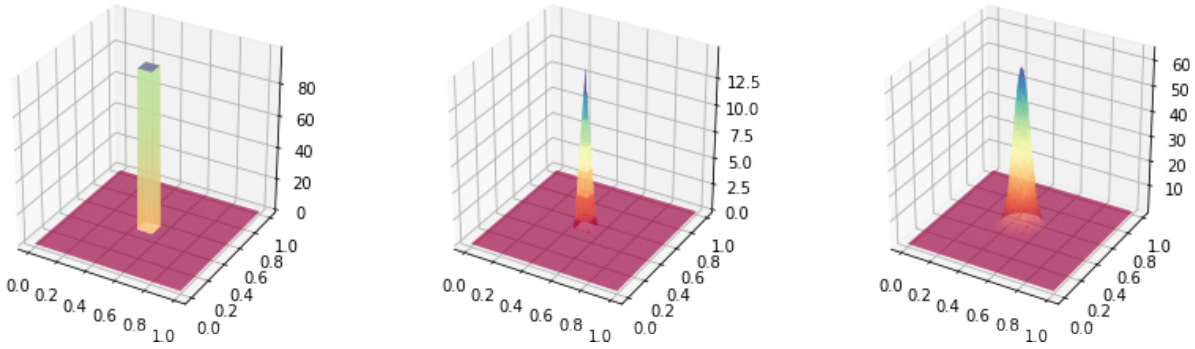

Figure 2: Different delta function approximations.

3 Numerical Methods

3.1 Finite element method

The finite element method (FEM) approximates the solution with a set of piece-wise smooth functions over the domain, which is divided into finite elements. These elements were chosen to be equally spaced quadrilateral elements. The basis chosen is piece-wise linear Lagrange polynomials, and polynomial interpolation is performed on each element. Numerical integration is performed using Gauss-Legendre quadrature of order n that integrates exactly polynomials of order $p = 2n - 1$. Since the function $f(x, y)$ that we are integrating is rather complicated and not just a simple polynomial, a very large quadrature rule (10) is used to ensure the quadrature error does not pollute the error of the solution.

The derivation of the weak form is as follows:
Find $u \in \Omega = [0,1] \times [0,1]$ such that for $f(x,y) = \delta(x - 0.5,\ y - 0.5)$, we have

$$-\Delta u = f \quad \forall\, x, y \in \Omega$$

and

$$u = 0 \quad \forall\, x, y \in \partial\Omega.$$

Defining the set of trial functions $\mathcal{S}$ and the set of test functions $\mathcal{V}$:

$$\mathcal{S} := \{u \in \mathcal{H}^2(\Omega) \mid u = 0 \quad \forall\, x, y \in \partial\Omega\}$$
$$\mathcal{V} := \{v \in \mathcal{H}^1(\Omega) \mid v = 0 \quad \forall\, x, y \in \partial\Omega\}$$

The method of weighted residuals states:

$$R(x,y) = \Delta u + f, \quad \int_\Omega R(x,y) v \, d\Omega = 0 \quad \forall v \in \mathcal{V}$$

Find $u \in \mathcal{S}$ such that

$$\int_\Omega (\Delta u + f) v \, d\Omega = 0 \quad \forall v \in \mathcal{V}$$
$$\int_\Omega \Delta u v \, d\Omega = \int_\Omega f v \, d\Omega$$

Divergence Theorem:

$$\nabla \cdot (\nabla u v) = \Delta u v + \nabla u \cdot \nabla v$$
$$\Delta u v = \nabla \cdot (\nabla u v) - \nabla u \cdot \nabla v$$

$$\int_\Omega \nabla \cdot (\nabla u v) d\Omega - \int_\Omega \nabla u \cdot \nabla v \, d\Omega = -\int_\Omega f v \, d\Omega$$
$$\int_\Gamma v \nabla u \cdot \boldsymbol{n} \, d\Gamma - \int_\Omega \nabla u \cdot \nabla v \, d\Omega = -\int_\Omega f v \, d\Omega$$
$$\int_\Omega \nabla u \cdot \nabla v \, d\Omega = \int_\Omega f v \, d\Omega$$

Weak form: Find $u \in \mathcal{S} : a(u, v) = F(v), \quad \forall v \in \mathcal{V}$

where $a(u, v) = \int_\Omega \nabla u \cdot \nabla v \, d\Omega, \quad F(v) = \int_\Omega f v \, d\Omega.$

3.2 Fourier spectral method

In this project, we solve the equation as follows

$$\frac{\partial^2 u}{\partial x^2} + \frac{\partial^2 u}{\partial y^2} = f(x, y)$$

with boundary condition $u(x, 0) = u(0, y) = u(x, 1) = u(1, y) = 0$, and $f(x, y) = -\delta(x - 0.5)\delta(y - 0.5)$. For Fourier expansion, since the boundary value of u is 0, therefore

$$u = \sum_{k_x=1}^{\infty} \sum_{k_y=1}^{\infty} \tilde{u}_{k_x,k_y} \sin(\frac{k_x \pi x}{L_x}) \sin(\frac{k_y \pi y}{L_y})$$

$$f = \sum_{k_x=1}^{\infty} \sum_{k_y=1}^{\infty} \tilde{f}_{k_x,k_y} \sin(\frac{k_x \pi x}{L_x}) \sin(\frac{k_y \pi y}{L_y})$$

where

$$\tilde{u}_{k_x,k_y} = \frac{4}{L_x L_y} \int_0^{L_y} \int_0^{L_x} u(x, y) \sin(\frac{k_x \pi x}{L_x}) \sin(\frac{k_y \pi y}{L_y}) dx dy$$

Therefore,

$$\begin{aligned}
&\sum_{k_x=1}^{\infty} \sum_{k_y=1}^{\infty} \tilde{f}_{k_x,k_y} \sin(\frac{k_x \pi x}{L_x}) \sin(\frac{k_y \pi y}{L_y}) \\
&= f(x, y) \\
&= (\frac{\partial^2}{\partial x^2} + \frac{\partial^2}{\partial y^2}) u \\
&= \sum_{k_x=1}^{\infty} \sum_{k_y=1}^{\infty} -[(\frac{k_x \pi}{L_x})^2 + (\frac{k_y \pi}{L_y})^2] \tilde{u}_{k_x,k_y} \sin(\frac{k_x \pi x}{L_x}) \sin(\frac{k_y \pi y}{L_y})
\end{aligned}$$

and

$$\tilde{u}_{k_x,k_y} = -\frac{\tilde{f}_{k_x,k_y}}{(\frac{k_x\pi}{L_x})^2 + (\frac{k_y\pi}{L_y})^2}$$

In this project, we use Gaussian distribution function to represent δ function. Gaussian distribution used in this project is as follows.

$$\frac{1}{2\pi\sigma^2}\exp[-\frac{(x-0.5)^2+(y-0.5)^2}{2\sigma^2}]$$

To guarantee accuracy, σ should be far larger than Δx. To make sure boundary condition is well satisfied, σ should also be far less than 1.

3.3 Finite difference method

Finite difference method is basically putting equally spaced grid points on the domain, and approximating the derivatives of the functions with the difference of local and adjacent points. This method is straightforward and easy to program, but it has some disadvantages: it has generally low order convergence rate, and it is not compatible with complex geometry.

For

$$\frac{\partial^2 u}{\partial x^2} + \frac{\partial^2 u}{\partial y^2} = f(x,y)$$

where $x \in [0,1], y \in [0,1]$. Discretize $[0,1]$ into N intervals. Then the 2-D plane is shown as follows. And the domain has $(N+1)\times(N+1)$ nodes.

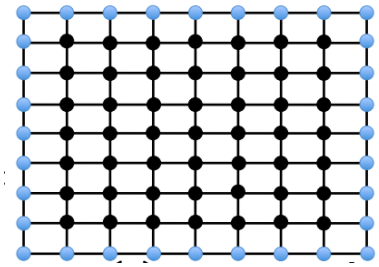

If interval distance of x direction and y direction is the same and the distance is h, then the second-order derivative of node (i,j) is

$$\left(\frac{\partial^2 u}{\partial x^2} + \frac{\partial^2 u}{\partial y^2}\right)_{i,j} = \frac{u_{i+1,j} + u_{i,j+1} + u_{i-1,j} + u_{i,j-1} - 4u_{i,j}}{h^2}$$

where, the coordinate of node (i,j) is (ih, jh).
Therefore, the Poisson's equation can be written as

$$\frac{u_{i+1,j} + u_{i,j+1} + u_{i-1,j} + u_{i,j-1} - 4u_{i,j}}{h^2} = f(x_i, y_j) = f_{i,j}$$

Let $\boldsymbol{L}$ be the Laplacian operator on $(N+1)\times(N+1)$ discrete field. Let F be the mapping from $(N+1)\times(N+1)$ index to $(N+1)^2\times 1$ index. Therefore $u_{i,j}$ in $(N+1)\times(N+1)$ array would be regarded as an element of $(N+1)^2\times 1$ vector $\tilde{u}_{F(i,j)}$. And the Laplacian operator can be written as an $(N+1)^2\times(N+1)^2$ large matrix $\tilde{L}$ which satisfies $\tilde{L}_{F(i,j),k}\tilde{u}_k = (\boldsymbol{Lu})_{i,j}$.

Let $\boldsymbol{e}^{i_0,j_0}$ be the discrete field being 1 at (i_0,j_0) and zero at other points, that is $(e^{i_0,j_0})_{ij} = \delta_{i,i_0}\delta_{j,j_0} = \delta_{F(i,j),F(i_0,j_0)}$. Then $(\boldsymbol{Le}^{i_0,j_0})_{i,j} = \tilde{L}_{F(i,j),k}\delta_{k,F(i_0,j_0)} = \tilde{L}_{F(i,j),F(i_0,j_0)}$. Therefore the $F(i_0,j_0)$-th column of $\tilde{L}$ is the $(N+1)^2\times 1$ form of $\boldsymbol{Le}^{i_0,j_0}$.

3.4 Chebyshev spectral method

Chebyshev spectral FEM is similar to the regular FEM except that instead of Lagrange polynomials, piecewise Chebyshev polynomials are selected as a basis, and instead of interpolation, Chebyshev expansion is performed on each element. Chebyshev expansion, considering one element, has exponential convergence rate as more bases are used, so Chebyshev FEM is expected to have a higher convergence rate compared to regular FEM.

The differential operator in the real domain is a matrix operation in the spectral domain. Consider that a function $A(x) = \sum_{n=0}^{M} a_n T_n(x)$, where $T_n(x)$ are Chebyshev polynomials. The derivative can be written as $A'(x) = \sum_{n=0}^{M} a_n T_n'(x) = \sum_{n=0}^{M} b_n T_n(x)$, and $\{b_n\} = [D]\{a_n\}$, or

$$\begin{pmatrix} b_0 \\ b_1 \\ b_2 \\ \vdots \\ b_{M-1} \\ b_M \end{pmatrix} = [D] \cdot \begin{pmatrix} a_0 \\ a_1 \\ a_2 \\ \vdots \\ a_{M-1} \\ a_M \end{pmatrix}$$

where

$$[D] = \begin{pmatrix} 0 & \frac{1}{2} & 0 & \frac{1}{2} & 0 & \cdots \\ & 0 & 1 & 0 & 1 & \cdots \\ & & \ddots & \ddots & \ddots & \\ & & & 0 & 1 & 0 \\ & & & & 0 & 1 \\ & & & & & 0 \end{pmatrix} \cdot \begin{pmatrix} 0 & & & & \\ & 2 & & & \\ & & \ddots & & \\ & & & 2(M-1) & \\ & & & & 2M \end{pmatrix}$$

The Laplacian operator can be written as $[D] * [D]$ in spectral domain, and that operator can be used for Poisson's equation. Start with the 1D Poisson's equation written as $u_{,xx} = f(x)$, with the boundary condition $u(0) = 0, u(1) = 0$.
The basis functions are defined as $T_n(2x-1)$, so that the domain of the Chebyshev polynomials can be $[-1, 1]$.
To solve this equation in Chebyshev spectral method, the equation becomes a problem of solving a matrix.

$$[D^2]\{\hat{u}\} = \{\hat{f}\}$$

where $u(x) = \sum_{n=0}^{M} \hat{u}_n T_n(2x-1)$, and $f(x) = \sum_{n=0}^{M} \hat{f}_n T_n(2x-1)$. However, the matrix $[D^2]$ is not invertible and the last two rows are zeros. So the boundary condition should be imposed by adding two more equations.

$$u(0) = 0 = \sum_{n=0}^{M} (-1)^n \hat{u}_n$$

$$u(1) = 0 = \sum_{n=0}^{M} \hat{u}_n$$

For 2D Poisson's equation $u_{,xx} + u_{,yy} = f(x, y)$, and boundary conditions are $u(0, y) = u(1, y) = u(x, 1) = u(x, 0) = 0$. In this case, the Chebyshev expansion becomes $u(x) = \sum_{m,n=0}^{M} \hat{u}_{mn} T_m(2x-1) T_n(2y-1)$, and $f(x) = \sum_{m,n=0}^{M} \hat{f}_{mn} T_m(2x-1) T_n(2y-1)$.
The Laplacian operator becomes $[\nabla^2] = [D_x]^2 + [D_y]^2$, where $[D_x] = 2[D] \otimes [I]$, $[D_y] = [I] \otimes 2[D]$. The matrix equation then becomes

$$[\nabla^2]\{\hat{u}\} = \{\hat{f}\}$$

$$u(0, y) = 0 \Rightarrow \sum_{m=0}^{M} (-1)^m \hat{u}_{mn} = 0, \forall n$$

$$u(1,y) = 0 \Rightarrow \sum_{m=0}^{M} \hat{u}_{mn} = 0, \forall n$$

$$u(x,0) = 0 \Rightarrow \sum_{m=0}^{M} (-1)^n \hat{u}_{mn} = 0, \forall m$$

$$u(x,1) = 0 \Rightarrow \sum_{n=0}^{M} \hat{u}_{mn} = 0, \forall m$$

For Chebyshev FEM, the Chebyshev method is used in each element. Given that the domain of the element is $[x_a, x_b] \times [y_a, y_b]$, the Laplacian operator becomes $[\nabla^2] = [D_x]^2 + [D_y]^2$, where $[D_x] = \frac{2}{x_b - x_a}[D] \otimes [I]$, $[D_y] = [I] \otimes \frac{2}{y_b - y_a}[D]$.
Suppose there are N by N elements in the domain, the elements are labeled in the following order, with the left most being the first element 0 and upper right being the last element $N^2 - 1$.

$$\begin{bmatrix} N^2 - N & N^2 - N + 1 & \cdots & N^2 - 1 \\ \cdots & \cdots & \cdots & \cdots \\ N & N+1 & \cdots & 2N-1 \\ 0 & 1 & \cdots & N-1 \end{bmatrix}$$

Therefore, for the interior elements, the element should be connected to the neighbors.

$$u^e_{right} = u^{e+1}_{left} \Rightarrow \sum_{m=0}^{M} \hat{u}^e_{mn} = \sum_{m=0}^{M} (-1)^m \hat{u}^{e+1}_{mn}, \forall n$$

$$u^e_{top} = u^{e+N}_{bottom} \Rightarrow \sum_{n=0}^{M} \hat{u}^e_{mn} = \sum_{n=0}^{M} (-1)^n \hat{u}^{e+N}_{mn}, \forall m$$

4 Results

4.1 Finite element method

For $\sigma = 0.01$, the results using different N (number of interval) are shown in Figure 3. At least 32 elements on each side are needed in order to have an accurate solution.

Figure 4 shows the values of the peak of the solution versus N, converging to a value of about 0.62556491 with N=128, compared to a peak value of 0.92464438 using the analytical solution described in the introduction.
Using the approximated analytical solution, $\int_0^1 u(x, y = 0.25)dx = 0.068177746$ and $\int_0^1 u(x, y = 0.5)dx = 0.16830902$. The absolute value of the difference between the value of this integral using the analytical solution as opposed to FEM is plotted in Figure 5 with varying values of σ. The results show that there is not much of a difference between using σ smaller than 0.1 away from the point (0.5,0.5). However, near the peak, as the value of σ decreases, the result is much closer to that of the actual delta function, which is expected.

Figure 6 demonstrates that the error of the numerical solution approaches the analytical solution as $\sigma \to 0$ and as the number of elements increases.

To find the convergence rate of the method itself, the absolute value of the difference between $\int_0^1 u(x, y = 0.25)dx$ for N=128 and N was found. This error for different σ is plotted in Figure 7. The convergence of the method seems to be independent of σ.

The convergence rate should increase with the degree of Lagrange basis functions for smooth functions, but only degree $p = 1$ was used in this study. For higher-order elements with degree p, the convergence order can reach $q = p + 1$.

One necessary assumption on the PDE is that the problem has a solution that is sufficiently regular, as expressed by the number of derivatives it has. We define the Sobolev function spaces H^k of order k of all functions on Ω that have weak derivatives up to order k. The convergence order k of the FEM with Lagrange elements with degree p is then limited by the regularity order k of the PDE solution as $q \leq k$.

Thus $q = \min\{k, p + 1\}$. Using linear Lagrange elements, we need $u \in H^k$ with $k = 2$ to reach the optimal convergence order of $q = p + 1 = 2$. Thus when using the delta function explicitly, as opposed to the Gaussian approximation, a prediction for the convergence rate should be $q = 2 - d/2 = 1$.

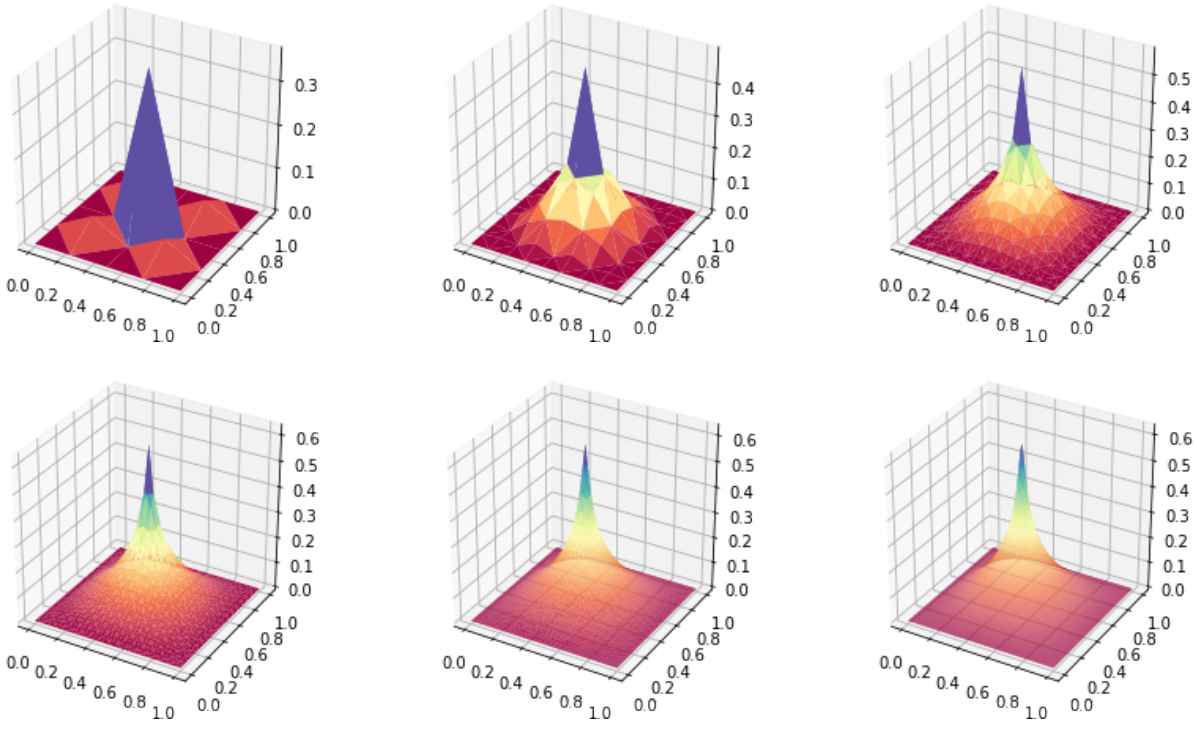

Figure 3: Numerical results for N= 4, 8, 16, 32, 64, 128 when $\sigma = 0.01$.

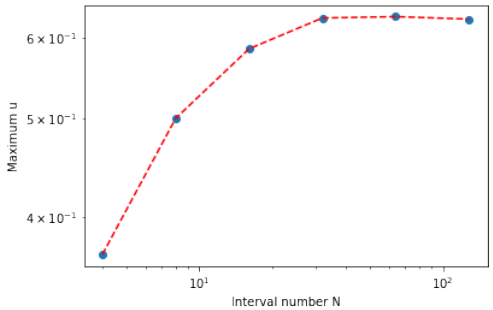

Figure 4: Maximum u converging as N increases, using a value of $\sigma = 0.01$.

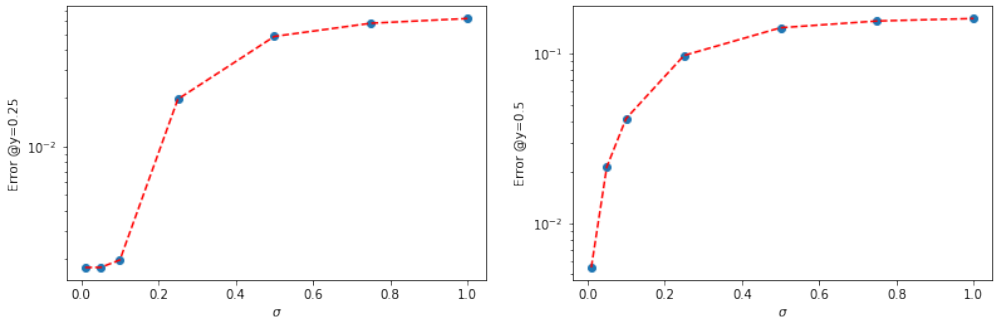

Figure 5: Using N=128, the error decreases as σ approaches 0.

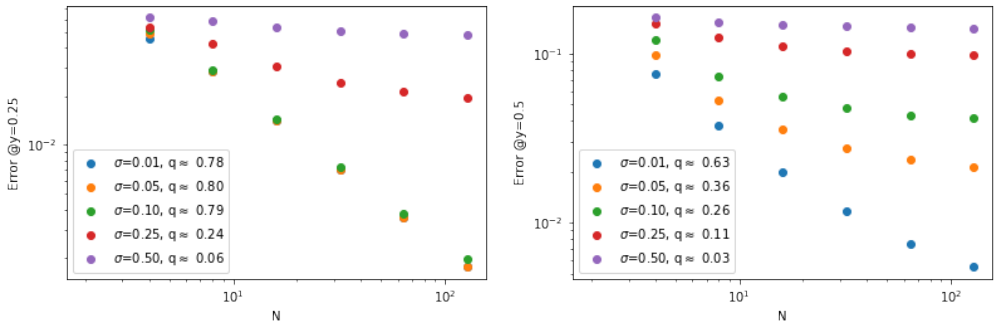

Figure 6: Convergence towards the analytical solution with varying σ and N.

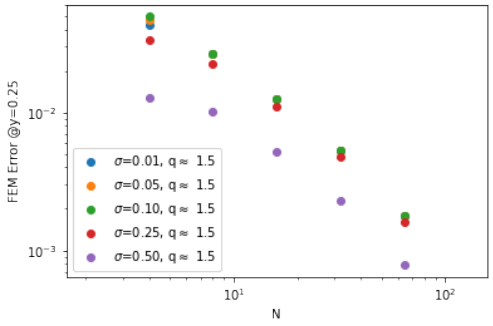

Figure 7: Convergence towards the FEM solution with varying σ and N.

4.2 Fourier spectral method

4.2.1 Solution for different N when $\sigma = 0.01$

For $\sigma = 0.01$, the result for different N (number of interval) is shown in Figure 8.

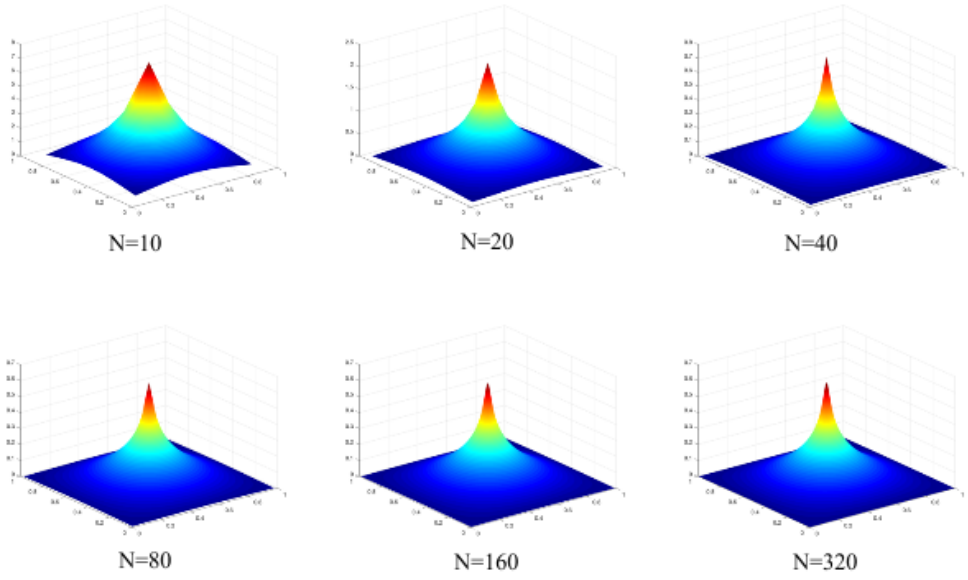

Figure 8: u values of different N when $\sigma = 0.01$

The plot of maximum u vs. N is shown in Figure 9. From the result, we can see that maximum value of u decreases when N increases. And the maximum u values converge to 0.62545 when N is larger than 80.

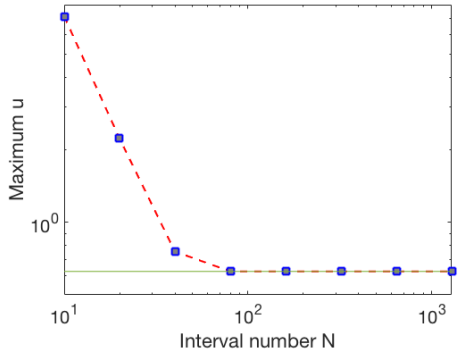

Figure 9: Maximum u vs. N (the green line is u=0.625450068823667)

4.2.2 Numerical accuracy and σ

In this section, set N=2000 to make sure that the solution convergent to a steady solution for a specific σ. From analytical calculation,

$$\int_0^1 u(x, y = 0.25)dx = 0.068184116$$

To analyze the relationship of numerical solution error and σ, we calculate the numerical value of $\int_0^1 u(x, y = 0.25)dx$ and compare that with analytical value. Numerical calculation error is defined as

$$abs\left[numerical(\int_0^1 u(x, y = 0.25)dx) - 0.068184116\right]$$

The semilog-plot of numerical calculation error vs. σ is shown in Figure 10. We can see that the numerical calculation error increases with σ increase. It's because Gaussian distribution becomes a bad approximation of δ-function when σ increases.

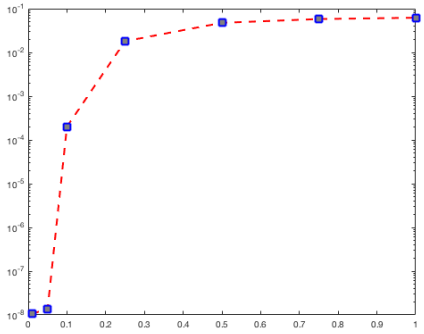

Figure 10: Semilog plot of numerical calculation error vs. σ

4.2.3 Convergence rate of numerical solution

To investigate the convergence rate, we define relative convergence error as

$$abs\left[\frac{\text{Numerical calculated centerpoint value @N} - \text{numerical convergent centerpoint value when N} \to \infty}{\text{numerical convergent centerpoint value when N} \to \infty}\right]$$

The plot of relative convergence error vs. N for different σ is shown in Figure 11.
From the calculation result, we can see that the convergent numerical maximum u decreases with σ increase. When σ is small (eg. 0.01 0.05), the convergence rate is large. But when σ is larger (eg. larger than 0.1), the convergence rate becomes smaller.

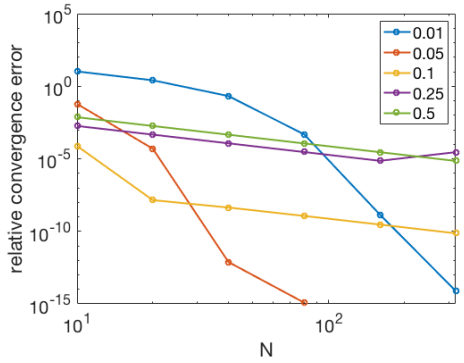

Figure 11: Relative convergence error vs. N for $\sigma = 0.01, 0.05, 0.1, 0.25, 0.5$

4.3 Finite difference method

4.3.1 Solution for different N when $\sigma = 0.01$

For $\sigma = 0.01$, the result for different N (number of interval) is shown in Figure 12.

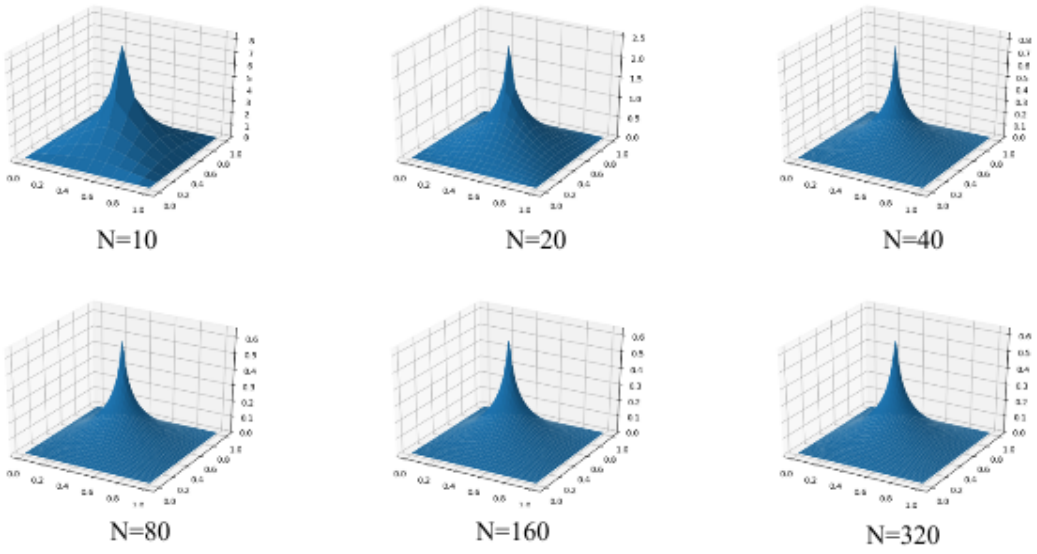

Figure 12: u values of different N when $\sigma = 0.01$

The plot of maximum u vs. N is shown in Figure 13. From the result, we can see that maximum value of u decreases when N increases. And the maximum u values convergent to 0.626 when N is 320.

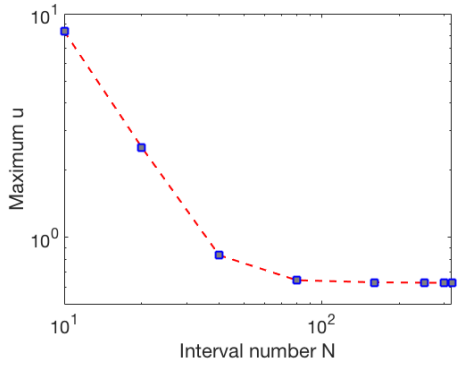

Figure 13: Maximum u vs. N when $\sigma = 0.01$

4.3.2 Numerical accuracy and σ

In this section, set N=320 to make sure that the solution well converges to a steady solution for a specific σ. From analytical calculation,

$$\int_0^1 u(x, y = 0.25)dx = 0.068184116$$

As discussed in 4.2.2, numerical calculation error is defined as

$$abs\left[numerical(\int_0^1 u(x, y = 0.25)dx) - 0.068184116\right]$$

The semilog-plot of numerical calculation error vs. σ is shown in Figure 14. We can see that the numerical calculation error increases with σ increase. It's because Gaussian distribution becomes a bad approximation of delta-function when σ increases.

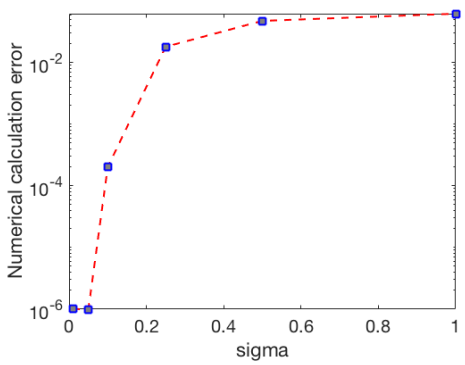

Figure 14: Semilog plot of numerical calculation error vs. σ

4.3.3 Convergence rate of numerical solution

Relative convergence error is defined in 4.2.3. The plot of relative convergence error vs. N for different σ is shown in Figure 14. We can see that the convergent rate is nearly the same for different σ when σ is larger than 0.05. But when σ is 0.01, the result converges faster than when σ is larger than 0.05.

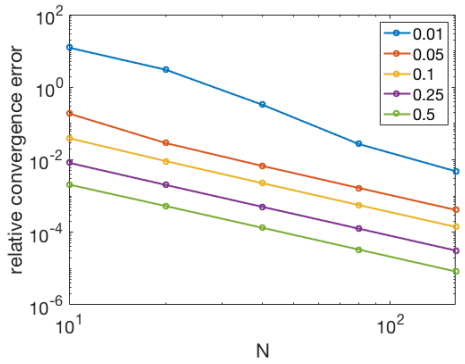

Figure 15: Relative convergence error vs. N for $\sigma = 0.01, 0.05, 0.1, 0.25, 0.5$

4.4 Chebyshev spectral method

Using the Chebyshev FEM method with polynomial order of 6, the numerical results of $\sigma = 0.01$ and $N = 10, 20$ are plotted in Figure 16. It can be observed that when $N = 10$, there are some unexpected perturbation around the center, and that is because the interpolation of the functions that are not so smooth can cause this wavy behavior. The $N = 20$ plots look smooth because the delta function is interpolated well if the grid size is small.

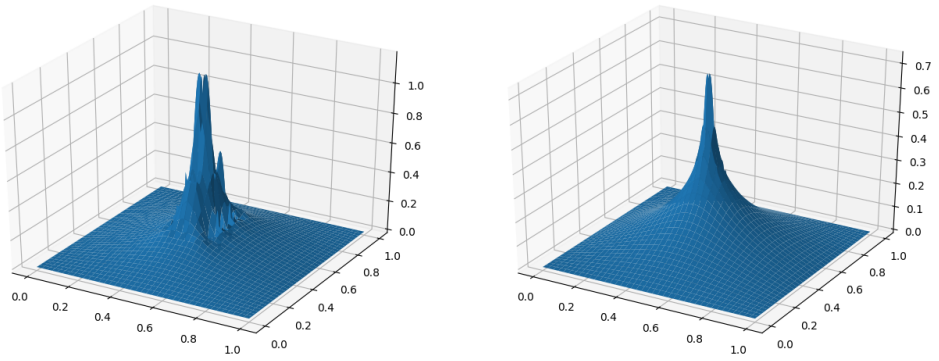

Figure 16: Numerical results for $\sigma = 0.01$, $N = 10, 20$

To find the error, I computed the result of $\int_0^1 u(x, y = 0.25)dx$ each time after the simulation, with the error computed relative to the most convergent result (N large enough). The convergence rate of Chebyshev FEM for different σ is plotted in Figure 17 using the polynomial order 6. This method has very high convergence rate, typically in the order of $O(N^{-6})$. If the source function is smooth, the solution converges even with a few number of elements. Even when $N = 10$, the error converges to a small number $O(10^{-8})$.

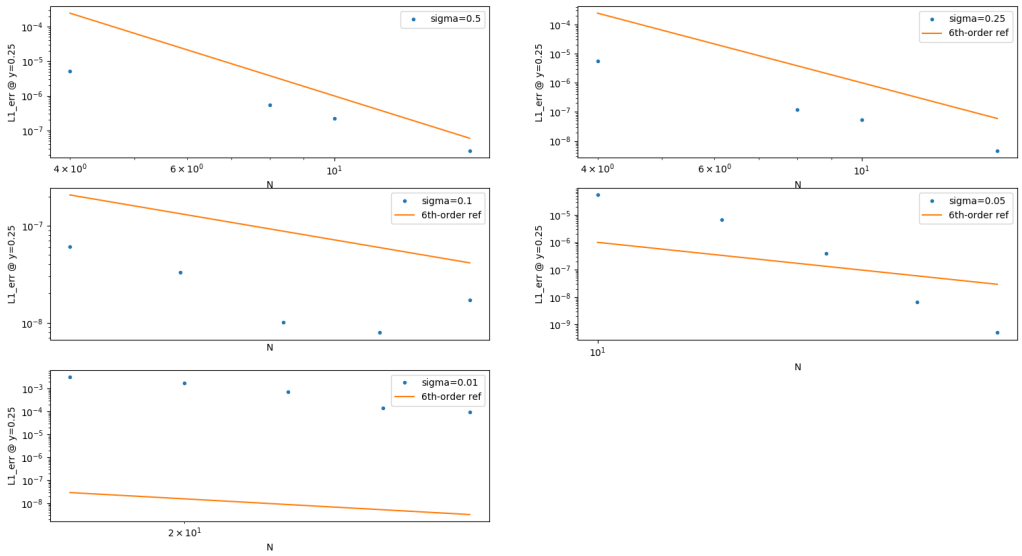

Figure 17: Convergence of each σ with respect to number of elements N

To evaluate how well the Gauss function approximate the delta-function, the error of $\int_0^1 u(x, y = 0.25)dx$ compared to the analytical solution is plotted with respect to σ. The error is good enough for $\sigma = 0.05$, but when σ gets smaller, the numerical solution becomes harder to converge.

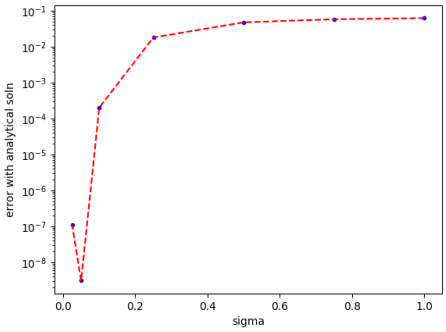

Figure 18: Convergence of each σ with respect to number of elements N

5 Conclusions

By comparing the different methods, the following similarities and differences can be observed from the numerical results, in terms of convergence rate and delta-function approximation:

1. It can be observed when the standard deviation of the Gauss function σ gets smaller, the results will approach the behavior of the delta function input, as shown in Figure 5, 10, 14 and 18.
2. The convergence rates are different in that the spectral and FEM generally have higher order convergence rate compared to finite difference.
3. An interesting phenomenon is that when σ gets smaller (the input function is not smooth), the convergence rate can be larger than the theoretical value.